A Computational Framework for Making Early Design Decisions in Deep Space Habitats

Amir Behjat*, Xiaoyu Liu† , Oscar Forero‡, Roman Ibrahimov §,
*Shirley Dyke¶, Ilias Bilionis‖, Julio Ramirez **, Dawn Whitaker††*

The dynamics of systems of systems often involve complex interactions among the individual systems, making the implications of design choices challenging to predict. Design features in such systems may trigger unexpected behaviors or result in large variations in safety, performance or resilience. To provide a means of simulating such systems for aiding in these decisions, we have developed a prototype tool, the control-oriented dynamic computational modeling tool (CDCM). The CDCM provides rapid simulation capabilities to perform trade studies in systems of systems. The general class of systems of systems that we aim to examine involve multiple hazards, damage, cascading consequences, repair and recovery. We especially focus on systems-of-systems that incorporate a health management system (HMS) that can monitor the state of the habitat and make decisions about actions to take. In this paper we describe the features of the CDCM, the architecture we devised for simulation of systems-of-systems, the unique functionalities of this tool, and we provide a demonstration of the capabilities by performing two illustrative examples. We articulate the use of this tool for making early design decisions and demonstrate its use for trade studies that consider a model of a deep space habitat. We also share some experiences and lessons that may be useful for others seeking to address similar problems.

Nomenclature

A_t	=	actions commanded by health management system
CP	=	collapse prevention
c_d	=	initial cost
d	=	design variables
d_b	=	battery mass

*Postdoctoral Researcher, School of Mechanical engineering, Purdue University
†Postdoctoral Researcher, School of Mechanical engineering, Purdue University, [Corresponding Author]
‡PhD student, School of Civil engineering, Purdue University
§PhD student, School of Aeronautics and Astronautics engineering, Purdue University
¶Professor, School of Mechanical engineering, Purdue University
‖Associate Professor, School of Mechanical engineering, Purdue University
**Professor, Lyles School of Civil engineering, Purdue University
††Associate Director, Indiana Space Grant Consortium

d_n	=	nuclear plant and fuel mass
d_s	=	solar panel mass
d_π	=	decision-making parameters
$E_{\text{bat.}}$	=	battery energy density
ENPV	=	expected valueof the net value
IO	=	immediate occupancy
LS	=	life safety
m_{Topaz}	=	Topaz nuclear plant mass
m_{base}	=	solar panel base mass
$P_{\text{nucl.}}$	=	nuclear power per nuclear fuel
P_t	=	interior environment pressure
t	=	time
P_{panel}	=	energy generated per solar panel
PGA_t	=	peak ground acceleration of the earthquake
$P_{i,j}$	=	probability to change the state from i to j after earthquake
RNPV	=	standard deviation of the net value
$r_{astronaut}$	=	hourly value for astronaut research
r_{launch}	=	cost of rocket launch
r_o	=	initial rebar radius
$t_{\text{Li-ion}}$	=	battery life
t_c	=	rebar degradation starting time
t_f	=	final time
t_{mission}	=	mission length
T_t	=	interior environment temperature
U	=	interdependent states
V	=	net value metric
v	=	value metric
X_t	=	states value
Y_t	=	observations
β	=	discount factor
Θ	=	physical parameters
θ_c	=	rebar degradation rate

π = decision-making policy

Ω = disturbances

Ω_1 = dust deposition rate

Ω_2 = solar irradiation

Ω_3 = lunar surface temperature

$\Omega_4^{\text{loc.}}$ = dome section stroke by meteor

$\Omega_4^{\text{inten.}}$ = meteor strike damage

Ω_4^{rate} = meteor strike rate

Subscripts

t = time

i = subsystem number

I. Introduction

Exploring space is essential for the economy [1], scientific advancement [2], and, most importantly, for the preservation of human life [3, 4]. As NASA and its affiliates express renewed interest in establishing a long-term human presence on the Moon, research into the development of long-term habitats has become a priority [5]. This has been motivated by various national and global reasons [6]. One critical area of focus in current space research is investigating the creation of habitat systems for extraterrestrial environments [5, 7, 8]. Due to the high cost of developing space habitats [7], even though low-cost ideas are being explored [9], it is crucial to use simulation tools to evaluate the effectiveness of designs before embarking on a mission [10]. It should be noted that physical testing of habitats may not be feasible due to the high costs or impracticality of creating realistic testing conditions [11, 12].

To understand the intricate interactions between the multiple systems within a space habitat and their collective impact on overall performance, requires knowledge of systems-of-systems modeling and simulation. Research efforts have methodologically explored these complex systems-of-systems. Fundamental guidelines for modeling and simulation are summarized in the literature, providing support for relevant studies [13–16]. In the context of systems-of-systems, principles are proposed for constructing studies in various of fields. This body of work collectively advances our capability to design and operate complex systems-of-systems [17–20]. Moreover, the attributes of interest in these systems-of-systems define the scope of the studies, including, for instance, safety, performance, or resilience. By constructing these models, performing simulations, and analyzing the outcomes, evidence can be extracted to assist decision makers. Studies also have been carried out to consider these attributes for various systems-of-systems [21, 22].

Several analogs have been developed to consider questions involving space habitats and their subsystems [23]. There are physical simulators like the NASA Habitat Demonstration Unit [12] or HERA [24]. There are also virtual simulators

like the Resilient Extra-Terrestrial Habitats institute's (RETHi) Modular Coupled Virtual Testbed (MCVT), which are built upon a collection of medium-fidelity dynamic subsystem models [8]. TRICK is a C/C++ library developed by NASA [25] and is another example of this class of simulators that allow simulation of dynamic systems. This simulator is great for real-time simulation but is challenging to use for systems with multiple components. There is also the well-known simulator ELiSSA [26] which was originally developed for Environmental Control and Life Support System (ECLSS) simulation for space flight. MELiSSA [27] also follows a similar idea to model a life support system. Each of these simulators provides specific capabilities to fully simulate the functions of a space habitat. Other notable works are open source software products like FIWARE [28] which is used to model energy management in buildings or OPEN [29] which is used for local energy management. These open software tools can also be used in various combinations to model a space habitat, but enabling that would require considerable modification. While there exist general-purpose dynamic system simulators such as Simulink (as documented in [30]), they are not free or open-access. Furthermore, some of them may not possess the user-friendly and flexible nature like Open Modelica (as described in [31]).

The majority of existing simulation tools are either not public or are designed for using physics-based models involving short-duration simulations. Therefore an open-source computationally efficient model with the flexibility to add new models and simulate complex systems is useful. This framework must be able to add or update the subsystems easily for users without forcing them to deal with the technical details of the simulation.

Compared to other commercial software[32], our work aims to provide an open-source tool that supports trade studies and maintains ease of use, while also highly customized and scalable for the modeling process. Our tool is designed from the bottom layer using Python to leverage the vast amount of knowledge and library available in Python communities, and to provide ready access to machine learning methods.

This paper introduces a modular and computationally efficient framework we call the control-oriented dynamic computational model (CDCM) that is intended for efficient simulation of systems of systems such as deep-space habitats. It is developed with the goal to evaluate decisions and conduct trade studies needed in the early stages of design. The CDCM can account for the occurrence of disruptions, disturbances to the system, the damage resulting from these events, and the repair and recovery. Degradation of subsystems over time may readily be included in the models. The architecture of the tool is first described along with the standard notation that is used to describe the dynamic equations of each subsystem. Then the framework is demonstrated using two illustrative examples of different complexities. The first example considers terrestrial structures experiencing both degradation and seismic inputs, and we generate an ensemble of data to find a suitable maintenance policy. The second example considers a system of systems model of a space habitat and addresses choosing a power subsystem configuration. Finally, while the framework has been developed with space habitat system of systems modeling in mind, its flexibility means that one can use it to simulate a broad set of complex systems.

The remainder of this paper is organized as follows. Section II presents the architecture of the framework. Sections

III and IV discuss two illustrative examples of increasing complexity to demonstrate the approach and provide results, and a discussion of how to select the appropriate design decision. Finally, concluding remarks are provided in section VI.

II. Technical Approach

A trade study is a systematic comparison between two or more candidate design alternatives. Often trade studies are performed in the early stages of the design process [33]. We want to perform trade studies based on rapid simulations involving systems of systems models [34]. Rapid simulation is characterized by two aspects, (1) the configuration setup is straightforward, and easy to model and expand (or scale), (2) the processing time of each simulation is short. Adopting a simulation-based approach allows one to consider the complex interconnections that occur among the various subsystems. Moreover, this approach facilitates including disruptions and their consequences, interventions to restore functionality, and system recovery in the simulations. When all of these factors need to be included in simulations, closed form equations that simply model their dynamics and performance are not generally available, especially because analytical uncertainty propagation [35] methods are often intractable in such systems. Thus simulations are needed to objectively and systematically consider the performance of a system of systems and several design alternatives.

The CDCM is suitable for rapid simulation of these classes of systems of systems to support trade studies [36, 37]. A diagram of the architecture of the code is provided in Figure 1. Four modules are included, denoted as: the configuration module, the system definition module, the simulation module, and the system output module. The overall concept is that the core of the code is used to both define the system of systems that is to be simulated, and to execute the simulations efficiently. Pre-processing takes place in the configuration module, and includes defining the system parameters that are to be varied, the ranges of those parameters, the metrics to be used for assessment, and the number of realizations to be performed. Post-processing takes place in the system output module, and includes logging the results of each realization, calculation of performance metrics, and data visualization. Each of these modules will be discussed in detail in the subsequent subsections.

A. Configuration Module

The configuration module comes first in the workflow and defines the scope of the trade study. It is a wrapper for the other three modules. A pool of candidate system configurations must be defined by identifying the subsystems to be included, their inter-dependencies, and the associated design parameters. The ranges over which these system parameters are to be varied must be defined, as well as the costs associated with each parameter choice. When fully defined, this pool of candidates describes the set of system-level configurations that are to be examined, or simulated.

In the current version of the code, each system configuration, once defined, is not random. Disturbances and disruptions may be modeled as stochastic or deterministic, depending on the scope and goals of the trade study. Here we

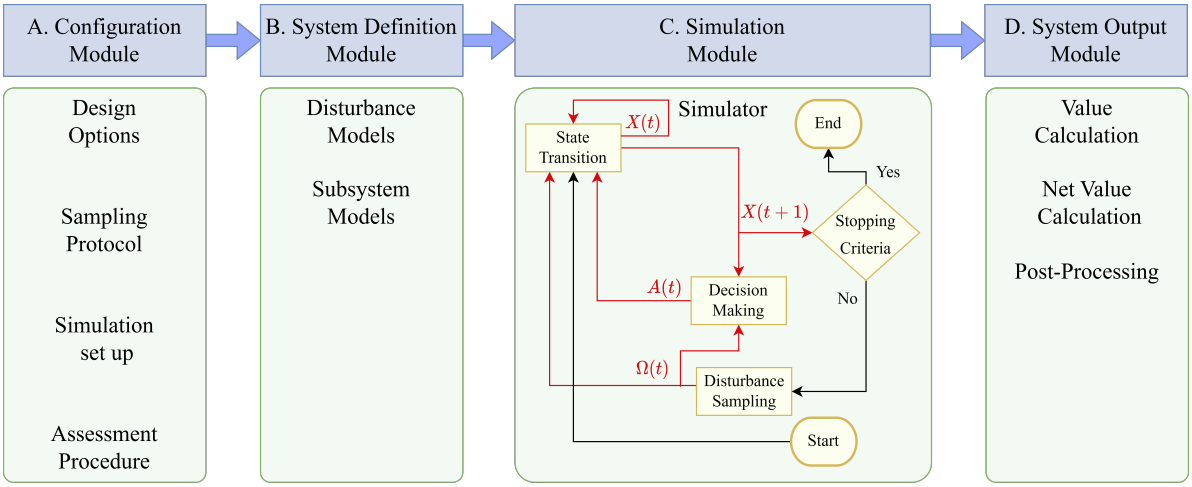

Fig. 1 Architecture of the CDCM Framework

define a *disruption as an event that could cause the system to transition from a region of safe behavior (nominal state) to a region of unsafe behavior (hazardous state). A disruption is modeled as an instantaneous change in the value of any parameter or state in the dynamical system* [38]). Disruptions modeled as stochastic include those that vary in time of occurrence or intensity (for example, the magnitude and time of occurrence of a seismic event). We also define a *disturbance as an external input to the system that may or may not cause the system to transition from a region of safe behavior to a region of unsafe behavior depending on the current state of the system*. Disturbances modeled as deterministic include those that have a regular occurrence with known values (for example, the position of the Sun in the sky). Disturbances modeled as stochastic include those that typically have variations that can be described statistically (for example, the deposition of dust). Alternatively one could provide a file with the time history of the disturbance. The sampling method used for each of these can be random, such as full factorial sampling [39], or a guided sampling approach such as Bayesian optimization [40].

B. System Definition Module

The second module is used to define both the appropriate models to be included in the system of systems, and how they fit together. Models must be defined for each disturbance and to transition the states for each subsystem. The code must also have the ability to trigger instantaneous changes in parameters or states in response to an event defined as a disruption. Initial values for each of the states must also be defined.

Transition models are typically dynamic equations that propagate each subsystem from one state at time t to the next time. Such state transition equations describe how the value of each state is to be updated based on the previous state values, any inputs, and time. These processes are assumed to be Markovian. If non-Markovian processes are to be used, the time history of the states should be considered part of the state. Disruptions and disturbances, defined in the previous section, may be modeled as either stochastic or deterministic, as discussed previously.

To ensure consistency between subsystems and support their connectivity, a standard notation is defined for the dynamic equations of each subsystem. We use t to denote the discrete simulation time, e.g., $t = 0$ is the initial time, and $t = 1$ the next time step. Suppose that we have N systems. We use $X_{i,t}$ to denote the state of system i at time t. The dynamics of system i are affected by the choice of the design parameters (d_i), the physical parameters (θ_i), any actions taken by the health management system ($A_{i,t}$), (potentially random) external disturbances (Ω_t), and inputs from other systems.

Let j be a system different than system i. The effect of j on i is captured through the coupling variables:

$$U_{j\to i,t} = h_{j\to i}(X_{j,t}).$$

In this notation, $U_{j\to i,t}$ is the empty set if there is no effect of j on i. Otherwise, $U_{j\to i,t}$ is a vector. The effect of all systems on system i is captured through the ordered tuple:

$$U_{-i,t} := \left(U_{j\to 1,t}, \ldots, U_{i-1\to i,t}, U_{i+1\to i,t} \ldots, U_{N\to i,t}\right).$$

We can now write the dynamics of system i as:

$$X_{i,t+1} = f_i(X_{i,t}, A_{i,t}, U_{-i,t}, \Omega_t, t; \theta_i, d_i), \tag{1}$$

where f_i is a suitably chosen function.

Notice that the equation above can describe both deterministic and stochastic Markovian dynamics. In the latter case, one would have to infuse any stochasticity through Ω_t. In addition, the formulation is sufficiently general to account for the case of memory by enlarging the dimensionality of the state.

In what follows, it is convenient to refer to the state of all systems collectively by $X_t = (X_{1,t}, \ldots, X_{N,t})$. Similarly, we define the actions vector, $A_t = (A_{1,t}, \ldots, A_{N,t})$, the design parameters, $d = (d_1, \ldots, d_N)$, and the physical parameters, $\theta = (\theta_1, \ldots, \theta_N)$. Under this notation, the dynamics of the state of all systems can be written as:

$$X_{t+1} = f(X_t, A_t, \Omega_t, t; \theta, d), \tag{2}$$

where the function f can be easily inferred from Eq. (1).

Let Y_t denote the observations one may be able to collect from the system. Mathematically, these observations are a function:

$$Y_t = g(X_t, A_t, \Omega_t, t; \theta, d). \tag{3}$$

This formulation can account for noisy measurements through the effect of Ω_t. We denote all the data collected up to time t by:

$$Y_{0:t} = (Y_0, Y_1, \ldots, Y_t).$$

The actions A_t of the health management system can only depend on the observed data through a policy function π, i.e.,

$$A_t = \pi(Y_{0:t}).$$

There are several challenges with the use of such a simulation framework. The first challenge is in selecting initial conditions for each of the states. Defining the appropriate initial values requires knowing the state that the system needs to start from to perform the desired trade study. Generally this would be a steady state condition to prevent start up transients that may lead to unintended perturbations in the system dynamics. Here we use a simple approach that involves running the code for a sufficiently large period to find appropriate initial values for each state. For more complex situations in which nominal values are not suitable, a systematic approach will be needed to set the initial state of the system. Another challenge in this type of study is in the selection of appropriate subsystem transition models to enable the scope and overall goals of the trade study to be achieved. For instance, the model to be used is linked with the time step needed. Physics-based models are often computationally demanding and require small time steps, making life cycle modeling quite time consuming. Thus, if such detailed models are not necessary for a particular study, one should choose computationally efficient models that consider the relevant dynamics and behaviors. One solution to achieve this goal is using data-driven models that are trained using higher-fidelity models [41]. Other approaches may also be used within this framework, and this is a topic of ongoing research.

C. Simulation Module

The next module executes the simulation. The CDCM code is written in Python [42]. First the states are initialized based on the initialization method defined in the discussion of the previous module. Then the code applies updates to each state and appropriately samples the random variables where sampling is required. The states update in each time step using the state transition models. The transition process is synchronous for all systems and the time step is assigned by the user in the Configuration Module. In this approach, all states are updated based on the same previous state value. This approach helps with tracking the states and avoids increment of error. However, it may add time discretization error into the simulation.

The simulation is stopped when the user-specified stopping criteria are met. Possible stopping criteria include, but are not limited to, a fixed simulation duration or a discontinuation of functionality of the system. Until the chosen stopping criteria are met, all disruptions, interventions, and recovery processes are continued.

Challenges associated with the execution of discrete-time dynamic simulation are well known, and thus not discussed

in detail here. In general, the simulation must be stable at the time step selected, or a variable time step may be used. However, for this initial code we are using a fixed time step that the user must define. As mentioned earlier, the decomposition of the system of systems can affect the results due to delays in propagating the states forward in time. Here we minimize the impact of this decomposition by selecting a smaller time step, although this is a topic that requires more attention.

D. System Output Module

The final module is used for storing the results and performing the calculations needed to obtain values for the chosen metrics. We assume that the system is intended to operate over a finite time horizon t_f. Here all simulation results are output and stored to enable the user to analyze the simulation time histories for computing the value metrics and their statistics. The code provides a means to then evaluate design configurations based on multiple simulation results, and to compare the value metrics for different design configurations to perform the intended trade study.

We use the term performance to refer to the ability of the system to function as intended. Performance has a wide variety of interpretations, depending on the stakeholder. A wide variety of performance metrics are available in the literature [43]. Those metrics that consider the consequences of disruptions, or damage, and recovery, or repair, are generally used in quantifying the resilience of a system [44, 45]. Although any metrics may be adopted when using the code, we recommend a performance metric that directly quantifies value and cost at each time step in the simulation.

Cost refers to the sum of the development, capital and operating costs for a particular configuration [46]. Whenever new technologies are being considered as alternatives, their development costs should be included in the performance metric. Otherwise, the cost of acquiring, installing and operating a given component that is selected is used. Thus, the cost of performing actions to recover from a disruption must also be quantified to properly assess cost, and therefore cost cannot be calculated in advance, rather it must be calculated for each realization based on the entire life cycle of the system.

We now provide a mathematical description of the performance metric described in this paper. Suppose that a given design configuration d has initial cost $c_0(d)$. Furthermore, let $v(X_t)$ be the value we enjoy (in the same units as the cost $c_0(d)$) if the system spends time step t in state X_t. Similarly, denote by $c(A_t, X_t)$ the cost of implementing action A_t when at state X_t. The value we gain (cost we incur) at time t is not necessarily directly comparable to the initial cost. To alleviate this issue we introduce the discount factor β, a number between zero and one. The idea is that a unit of value at time t is worth β^t units of value at the initial time step. The *net present value* of a trajectory $X_{0:t_f}$ (t_f is the final time) is defined to be:

$$V(d) = \sum_{t=1}^{t_f} \beta^t \Big(v(X_t) - c(A_t, X_t) \Big) - c_0(d). \tag{4}$$

In words, the net present value of a trajectory is the sum of all values minus the sum of all costs measured in terms

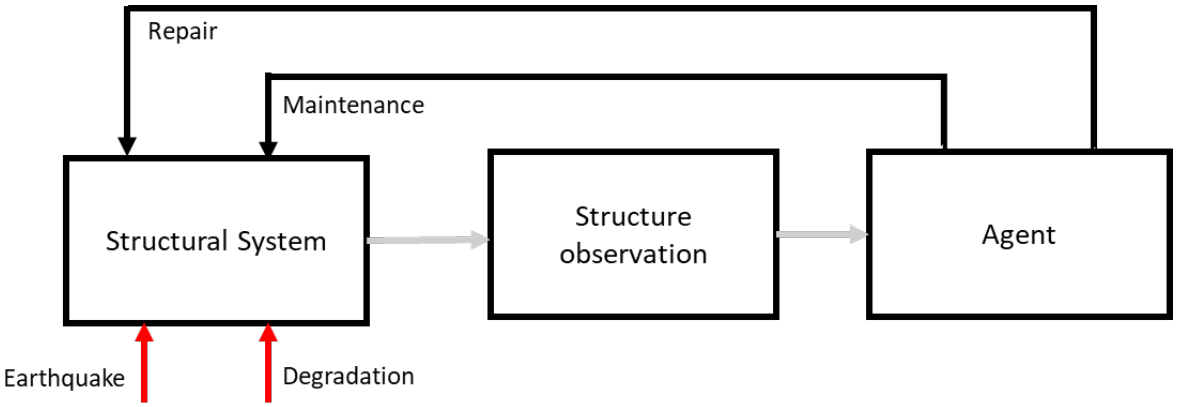

Fig. 2 Diagram of the Terrestrial Building Example.

of initial step value units. The main challenge in formulating this metric, is how to express the value and the cost in common units. The choice is application specific, as illustrated in the examples in Sections III and IV.

The net present value is a random variable because the trajectory is itself random. We perform trade studies using the statistics of the net present value. To this end, define the *expected net present value* of a design d by:

$$\mathrm{ENPV}(d) = \mathbf{E}\left[V(d)\right]. \tag{5}$$

The expectation is over all the random variables, i.e., the states X_t, the observations Y_t, and the external disturbances Ω_t. In practice, we use a sampling average approximation to this expectation. Another useful metric is the standard deviation of the net present value, i.e., the risk. It is defined by:

$$\mathrm{RNPV}(d) = \sqrt{\mathbf{V}\left[V(d)\right]} = \sqrt{\mathbf{E}\left[V(d) - \mathrm{ENPV}[V(d)]\right]}. \tag{6}$$

III. Illustrative Example I: Terrestrial Structural Performance with Aging and Repair

We demonstrate the framework by studying the lifecycle of a typical terrestrial building when subjected to both degradation due to aging and random seismic events. The system consists of one subsystem, a 3-story reinforced concrete frame building located in the Los Angeles area, and is representative of modern engineering practices in zones with a high seismic hazard ([47, 48]). The building is designed to have an expected service life of 100 years.

Damage can be produced in two ways, a loss of cross-section in the steel rebar due to corrosion, and the damage due to earthquakes. Ground motions are considered to be a disruption, and the occurrence of a seismic event may cause the building to transition into a hazardous state. The building is also exposed to environmental factors over its lifecycle that will produce corrosion with age. This system is represented by the diagram in Figure 2.

Functionality is selected as the measure of value in this example. When the building is not damaged or it is in the

lowest level (zero to mild) of damage, it is fully functional and the value is based on the income generated. When the building is damaged mildly or moderately in an earthquake, it is assumed that it can be repaired (an action). However, if the event is large enough, the building is severely damaged and repair is not possible, and the structure cannot be occupied and thus loses functionality. The likelihood of the building transitioning to a damaged state increases with the level of corrosion at the time of a given seismic event. Maintenance (an action) can be performed to improve the condition of the building with regard to corrosion.

A. System Configuration

The system here includes a single building in a seismic zone. Two external factors are modeled in this system that can cause the system to change its state. Disruptions that may effect the system are earthquake events. Earthquakes are modeled as a random event here, and the model is based on data obtained from the CESMD for Los Angeles [49]. We use the peak ground acceleration, e.g. $\Omega_t = \text{PGA}_t$, to model its severity.

To generate a data-driven model of the building performance, a finite element model of a typical moment resisting frame in one of the two principal directions of the building is first developed using SAP2000 [50]. To generate this model the following assumptions are made: (i) fixed base for the columns, (ii) each floor slab acts as a rigid diaphragm, and (iii) cracked section stiffness for columns and beams as recommended in ACI 318-19 [51]. Ductility is modeled using typical assumptions for a frame in this class [48]. The mass is computed based on superimposed loads and the self-weight. The resulting finite element model of the typical moment resisting frame has 21 elements, 16 nodes, and 36 degrees of freedom. This finite element model is used to generate a data-driven model, in this case a fragility function. Fragility functions are a common tool for predicting damage level after a seismic event, as discussed later.

Buildings age over time. Aging and the associated degradation in buildings is primarily associated with the corrosion of the reinforcing bars. The states of the building are also affected by time, and corrosion is assumed to be deterministic here. The specific rate of section loss depends on variables that are related to the specific location of the building and the details of the structural elements.

The service life of a structure then can be divided into an initial period, before the corrosion initiates in the rebar, and the propagation period, during which the steel continues to degrade. A representative degradation function is selected having an initial period of 15 years with a rate of 0.003 in per year. For simplicity, degradation is assumed to increase linearly and uniformly for both the transverse and longitudinal reinforcement in the concrete member. At this rate the degradation alone will not cause the building to lose its functionality in the assumed 100-year service life.

B. System Definition

The system has three state components $X_t = (X_{1,t}, X_{2,t}, X_{3,t})$: the effective rebar radius, $X_{1,t}$, the number of years passed since the last maintenance $X_{2,t}$, and the earthquake state $X_{3,t}$. The former two capture the effect of continuous

structural degradation. The latter captures the effect of earthquake events on the structural integrity of the building. The action variable also has two components $A_t = (A_{1,t}, A_{2,t})$. The first action component, $A_{1,t}$, is associated with maintenance. The second action component, $A_{2,t}$, models earthquake damage repairs. The time step we operate on is one month, i.e., $\Delta t = 1$ month.

The dynamics of the effective rebar radius are deterministic. Let r_0 be the initial rebar radius in inches, i.e., $X_{1,0} = r_0$. For the first $t_c = 15$ years no corrosion occurs. After this period, corrosion occurs at a constant rate $\theta_c = 2.5 \times 10^{-4}$ in/month. When maintenance occurs, with a fixed occurrence period of t_m, $A_{1,t} = 1$, it returns $X_{1,t}$ to the initial value r_0. Maintenance does not occur when $A_{1,t} = 0$. Mathematically, the dynamics are given by the following equation:

$$X_{1,t+1} = \begin{cases} r_0, & \text{if } t \le t_c, \\ \min\{X_{1,t} - \theta_c \Delta t, 0\}, & \text{if } t > t_c, \text{ and } A_{1,t} = 0, \\ r_0, & \text{if; } t > t_c \text{ and } A_{1,t} = 1. \end{cases} \tag{7}$$

The dynamics of $X_{2,t}$ are also deterministic. They are:

$$X_{2,t+1} = \begin{cases} X_{2,t} + 1, & \text{if } A_{1,t} = 0, \\ 0, & \text{if } A_{1,t} = 1. \end{cases} \tag{8}$$

We now discuss the maintenance policy. The policy is based on observations $Y_{1,t} = X_{1,t}$. We initiate maintenance whenever the observed effective rebar radius $Y_{1,t}$ is less than 75% of the initial value. Mathematically:

$$A_{1,t+1} = \pi_1(Y_{1,1:t}) = \begin{cases} 1, & \text{if } t \bmod t_m = 0, \\ 0, & \text{otherwise.} \end{cases} \tag{9}$$

The earthquake state $X_{3,t}$ takes four different discrete values ranging from 1 to 4. The value 1 corresponds to a healthy building. Values 2, 3, and 4 correspond to different seismic performance codes as summarized by ASCE 41-17 [48]. Specifically: 2 – immediate occupancy (IO), the structure is minimally damaged; 3 – life safety (LS), the building is not a safety threat and damage can be repaired; 4 – (CP), the building is damaged beyond repair.

The dynamics of the quake state $X_{3,t}$ are stochastic. The transition probabilities depend on the rebar radius $X_{1,t}$ and on the seismic intensity $\Omega_{1,t} = \text{PGA}_t$. To proceed we need to model the conditional probabilities

$$P_{ij}(r, a) = p(X_{3,t} = i | X_{1,t} = r, X_{3,t} = j, \Omega_{1,t} = a),$$

i.e., the probability of jumping from an earthquake state j to an earthquake state i, when the effective rebar radius is r

and we experience an earthquake with peak ground acceleration a. When no earthquake is occurring, $a = 0$, then these probabilities take the trivial form:

$$P_{ij}(r, 0) = \begin{cases} 1, & \text{if } i = j, \\ 0, & \text{otherwise.} \end{cases}$$

In other words, the earthquake state does not change if no earthquake happens. In case $a > 0$, these probabilities are typically called fragility curves/functions. We estimate the fragility curves using nonlinear static pushover (NSP) analysis [48]. In NSP, one generates synthetic seismic events, i.e., ground acceleration profiles, and propagates them through a finite element model of the building. In our case, we perform NSP for eleven different rebar radii values ranging equidistantly from the initial, r_0, to the minimum allowable radius, $0.75r_0$. Using the generated data, we fit the fragility curves to a parametric form.

Repair of earthquake damage occurs whenever the $Y_{2,t} = X_{3,t}$ has either the value 2 (IO) or 3 (LS). There is no possibility of repair when $Y_{2,t}$ has a value 4 (CP). Repair takes a total of six months. The earthquake repair action variable $A_{2,t}$ is coded as follows. We use the value 0 to indicate that no-repair is taking place. We use the value 1 to indicate that the repair is occurring. We use the value 2 to indicate that the repair will be completed in the next time step. So, the policy function is:

$$A_{2,t+1} = \pi_2(Y_{2,1:t}) = \begin{cases} 0, & \text{if } Y_{2,t} = 1, 4, \\ 1, & \text{if } Y_{2,t} \neq 1, 4 \text{ and there exists } s \in \{1, \ldots, 5\} \text{ such that } Y_{2,t-s} = 1, \\ 2, & \text{if } Y_{2,t-s} \neq 1, 4 \text{ for all } s \in \{1, \ldots, 5\}. \end{cases}$$

To state the dynamics of $X_{3,t}$ in the standard notation, we need to introduce an additional disturbance random process $\Omega_{2,t}$. The variables $\Omega_{2,t}$ are independent and uniformly distributed in $[0, 1]$. So, the external disturbance vector is $\Omega_t = (\Omega_{1,t}, \Omega_{2,t})$. The dynamics are:

$$X_{3,t+1} = \begin{cases} 1, & \text{if } A_{2,t} = 2, \\ i, & \text{if } \sum_{i'=1}^{i-1} P_{i',X_{3,t}}(X_{1,t}, \Omega_{1,t}) \leq \Omega_{2,t} \leq \sum_{i'=1}^{i} P_{i',X_{3,t}}(X_{1,t}, \Omega_{1,t}). \end{cases} \tag{10}$$

C. Discussion of Results

The goal of this study is to choose the most appropriate maintenance period for the structure. Figure 3a shows the ENPV vs. the RNPV. The maintenance frequencies we consider, most of which are annotated in the plot, are 1, 2, 3, 5, 8, 10, 12, 14, 16, 18, 20, 25, 30, 40, 50, 60, 75, 80, and 90 years and the case in which no maintenance is performed. One wants to choose an option that maximizes the ENVP and minimizes the RNPV.

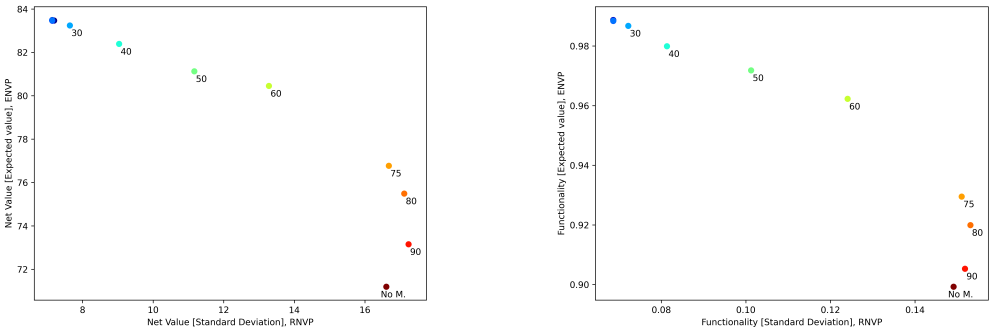

(a) ENVP **vs** RNVP **(b) Functionality: Mean vs standard deviation**

Fig. 3 Results for Example I: Building subjected to both aging and earthquakes, considering several maintenance period options

The results of this illustrative example indicate that the points with more frequent maintenance have, in general, a higher average value with less variability. This outcome occurs despite having a higher maintenance cost overall, due to the associated lower repair needs resulting in higher functionality. Less frequent maintenance also shows promising ENVP but results in higher RNVP, i.e., higher risk. These choices benefit from having lower maintenance cost while they also have lower functionality. The no-maintenance case is clearly dominated and should be avoided.

Figure 3b shows the distribution of the value, or functionality, of the building, over 1000 runs corresponding to each maintenance period considered in 3a. It is important to note how close the first few points are to each other. In other words, using a very low maintenance period adds little to the functionality while it increases the cost. The other points show there is a gradual decrease in functionality associated with less frequent maintenance.

Based on the results, choosing a maintenance period with a period below 30 years is most appropriate. These maintenance frequencies lead to similar results. One of the main reasons for this outcome is the importance of the repair costs compared to maintenance costs. The specific results will change for other buildings and conditions based on the relevant costs and income.

IV. Illustrative Example II: Extraterrestrial Habitat Simulation

To illustrate the use of the code, we define a sample space habitat system located on the Lunar surface and perform a trade study. This trade study is intended to demonstrate how the code facilitates making decisions during the early design phase of a project.

We investigate the influence of technology choices and selected design parameters on the overall system performance. We focus on identifying the most appropriate energy source for a space habitat over its lifecycle. In particular we compare solar panels, a nuclear plant, and a lithium-ion battery. The NVP encodes the fact that we wish to maximize the time that the space habitat has the required interior conditions throughout its lifecycle, over a large number of possible

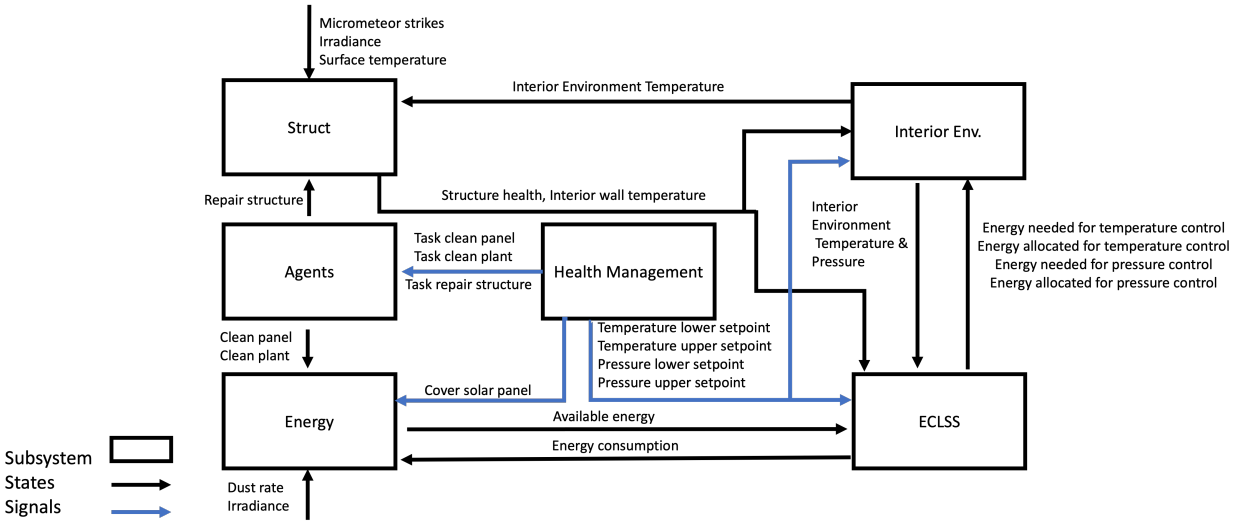

Fig. 4 Diagram of the Sample Lunar Habitat System Showing Interactions between Subsystems

realizations based on sampled disruptions (i.e., it is functional).

A. Description of the Sample Habitat System

Our sample habitat system includes a core set of essential subsystems. These include the structural subsystem, the power subsystem, and thermal and pressure management systems. The environmental conditions on the Lunar surface and disturbances to the habitat system are included within the *exterior environment model*. We assume the habitat is a hemisphere with a 2.9 m radius and the fixed parameters (those that are not varied to perform the trade study) are selected to be compatible with this assumption. We measure performance in terms of the ability of a the habitat to maintain life and provide the required interior conditions. So, we also need a model of the *interior environment*. When an intervention, such as removing the dust from the solar panels, is needed, the *robot agent model* is called to perform a task that is commanded by a very basic *health management system*. Figure 4 shows a schematic diagram of the habitat system. Habitat systems are shown as boxes and the arrows indicate the causal relations. In what follows we provide a brief description of each of the models.

Exterior Environment: Establishing and operating a deep space habitat on the Moon requires dealing with an environment that is more extreme than anywhere on Earth [8]. The exterior environment model consists of both the set of nominal conditions and the stochastic disturbance models that match our current understanding of the Lunar surface environment. Relevant models of the Lunar conditions include radiation [52] and temperature [53]. Pressure is taken to be 0 psi, vacuum. Disturbances considered include micrometeorite impact and dust accumulation. Table 1 describes the characteristics of the exterior environment model with solar radiation, dust accumulation, micrometeorite impact, and the external temperature and pressure. Here the temperature, pressure, and radiation are deterministic functions that are

Table 1 List of disturbances modeled in Example 2

Sampling Function	Description	Unit
dust accumulation	$\Omega_{1,t} \sim \text{Normal}(\mu = 1E-5,\ \sigma = 2.5E-6)$	$\frac{\%\ \text{area covered}}{\text{hr}}$
solar radiation	$\Omega_{2,t} = \frac{1450}{2}\Big(\sin(\pi t/(29.503 \times 12\ \text{hr})) + \lvert\sin(\pi t/(29.503 \times 12\ \text{hr}))\rvert\Big)$	$\frac{\text{W}}{\text{m}^2}$
external environment temperature	$\Omega_{3,t} = 100 + 150\Big(\sin(\pi t/(29.503 \times 12\ \text{hr})) + \lvert\sin(\pi t/(29.503 \times 12\ \text{hr}))\rvert\Big)$	K
micrometeorite impact rate	$\Omega^{\text{rate}}_{4,t} \sim \text{Poisson}(\lambda = 0.015)$	$\frac{1}{\text{hr}}$
micrometeorite dome damage	$\Omega^{\text{inten.}}_{4,t} \sim \text{Normal}(\mu = 0.3,\ \sigma = 0.3)$	% damage dome
micrometeorite impact location	$\Omega^{\text{loc.}}_{4,t} \sim \text{Categorical}\{1,\ 5\}$(Equal probability to hit all sections)	-

affected by Moon cycles (every 29.503 Earth days), while dust accumulation and micrometeorite impacts are stochastic. Note that this model does not have states.

Power Subsystem Model: All of the subsystems of the habitat require sufficient power to function properly. The power subsystem model governs the generation, storage, and distribution of power to the habitat subsystems. The power subsystem considers power can be generated through both solar panels and a nuclear plant. The generated energy is then stored in a battery, which has a pre-defined maximum capacity. Surplus power is discarded. Stored power is distributed as needed to the subsystems that are consuming power. The inputs from the external environment model are solar radiation and dust. Other inputs to this subsystem include the power consumed by other subsystems, specifically the temperature and pressure control subsystem. The solar panels can be covered, in which case they are not generating power or collecting dust. The model assumes the solar panels are covered during the Lunar night when solar radiation is zero. Thus, the control inputs to this subsystem include the command to cover the solar panels, and the command to clean the dust from solar panels or radiators. The four physical states of this subsystem are the condition of the solar panel (covered/uncovered), the power being generated by the solar panels, the power being generated by the nuclear plant, and the amount of energy that is currently stored in the battery. The power subsystem has two states related to the dust accumulated, one corresponding to the solar panels and the second corresponding to the radiators of the nuclear reactors. Each of these has a direct impact on the operation of the corresponding power generation methods. The parameters for this model are explained in detail in subsection IV.C. For detailed information about this subsystem model, please, see table 7 in the appendix.

ECLSS Subsystem: The ECLSS maintains a temperature and pressure that are within an acceptable range. In this study, thermal and pressure management are the only functions of ECLSS. Pre-determined set points are defined based on a range that is suitable to support the crew and are used to govern the operation of the thermal and pressure control systems. The inputs to this subsystem are the temperature in the interior environment, the pressure in the interior environment, the power stored, and the damage state of the structure. Clearly ECLSS draws power from the battery, and must have sufficient power to operate. The physical states of this system are the power consumed by temperature control, power consumed by pressure control, power needed by temperature control, and the power needed by the

pressure control. The thermal management system is modeled as a first-order system and is represented by a simple controller. A similar controller used to represent the pressure management system to represent the first order dynamics of this controller. This system is not directly affected by disturbances. However, disturbances indirectly decrease the energy generation or increase the thermal conductivity which does impact the performance of the ECLSS subsystem. Temperature control modules have a coefficient of performance which is designed based on the current models. The temperature control is assumed to have 12.5 coefficient of performance (Q/W) which is the ratio between the energy transferred to the room and the used energy to control the HVAC system. For the pressure control we only define the amount of energy required to increase 1atm pressure. This energy is different than the energy required to bring the oxygen tanks and it is assumed to be 31.25. Since the simulator uses a large time step, it is impossible to use high fidelity dynamics. So, instead of modeling the pressure and temperature directly, we model them based on the amount of energy can be used and the amount of the required energy. In other words we assume a steady state value with energy as the governing factor. Here, we consider the pressure control has priority to temperature control. Therefore, the energy is used to control the pressure first and if there is additional energy to control temperature, the temperature is also controlled. The outputs of this subsystem are the air and the heat that are provided to the interior environment. In the current example, the physical states of the ECLSS are not modeled. Having an accurate thermal model depends not only on conduction, but also on the convection coefficient of air, which is crucial for thermal control. Here the forced conductivity of the air is used as a basis of the model [54]. The other heat transfer method, radiation, affects the thermal flow to the dome. The parameters associated with this heat transfer method are emissivity [55], 0.9, and absorptivity [56], 0.60, which are chosen to be close to concrete. Note that some factors that also play a role in heat transfer are omitted in this demonstration. For instance, humidity and humidity management, the heat transfer across the boundary due to radiative transport, and the potential for heat imbalance caused by the varying energy required in the cooling and heating process are neglected in this simple habitat model. For detailed information about this subsystem model, please see table 8 in the appendix.

Structural Subsystem: Serving to provide thermal protection, pressure containment, and structural integrity, the structural subsystem can experience damage when a micrometeorite strike occurs on or near the habitat. The model used for the structure includes basic properties such as thickness and thermal conductivity. We represent the structure as five separate segments, any of which may be impacted and experience damage during a micrometeorite event. In this subsystem, damage is simulated by using a sampled event from the external environment model. The structural segments receive damage based on the strike location and the amount of energy released (mass and velocity). The inputs to this system include the external temperature, external pressure, solar radiation, and micrometeorite impacts. The physical states of the structural subsystem model include the temperature of the structure on both the interior and exterior surfaces. Micrometeorite strikes are the source of health degradation of the structural subsystem. The repair procedure uses agents to improve the health of the structural segments, and the repair of each segment is the control

inputs to this subsystem model. The damage state of the structural subsystem model conveys how intact the structural dome is, and depends on: 1) its damage health state at the previous time step, 2) the degree of damage due to any recent micrometeorite impacts, and 3) actions taken for repair by the agent. The outputs of this subsystem are the temperature and pressure at the interior surface of the structure. For more details, please, see Table 5 in the appendix. The parameters associated with this system include the nominal and damaged conductivity coefficient which are chosen based on values that correspond to reinforced concrete [57]. When damaged, the structure may lose up to 95% of its thermal isolation as compared to the undamaged structure. The heat conductivity of the wall changes with damage using an initial user specified thickness, 0.2 m, and structure is assumed to a radius of 2.9 m.

Interior Environment: The conditions inside the habitat are described by the interior environment model. This model has two physical states: temperature and pressure. The inputs to the model include the temperature of the interior of the structure, and the heat added by the thermal management system, as discussed in the next section, pressure added by the pressure management system as well as the damage state of the structure. The physical states are thus updated at each time increment based on these inputs and the set points defining the acceptable temperature ranges from the health management system. While ECLSS aims to control both the temperature and pressure based on the setpoints, the internal environment model is used to track these changes. For more information, please, see table 9 in the appendix.

Health Management System: The brain of a space habitat is the health management system (HMS). The system is designed under the assumption of perfect information and optimal task execution through an agent. The HMS has two functions: to synthesize the results of *fault detection and diagnosis* (FDD) algorithms coming from the subsystems, and to perform *decision-making* (DM). The system assumes that faults are detected and diagnosed perfectly, and a decision to repair a fault is made using that data in one time step. The HMS is provided the state of each subsystem as inputs. The outputs are commands to the agents as shown in table 2 and discussed in the next paragraph. Commands may also be sent to the power subsystem to cover the solar panels. The HMS is also responsible for commanding the set point for the thermal and pressure management functions of the ELCSS subsystem in this sample habitat. In this illustrative example, we assume that the HMS knows the true states of the relevant subsystems and makes perfect decisions regarding interventions.

Agent Model: The agent model is very simple for this trade study. The agent is used to execute a commanded action requested by the HMS. The inputs to this subsystem are the commands, and the outputs of this subsystem are the confirmation that the action has been completed. We also assume the agent can deliver all the commands made by the HMS perfectly. However, the completion rate of tasks does not allow it to finish it instantly. For more detail, see table 2.

B. Trade Study: Choosing the power generation system

We focus on choosing the technologies and approximate design parameters for the power subsystem. The relevant design parameters in this study are power storage capacity, the total area of the solar panels, and nuclear reactor nominal

Table 2 HMS decision-making rules used in example 2

Action name	Condition to activate the actions	Competency time
cover solar panel surface	solar irradiation = 0	instantaneous effect
clean solar panels	solar panel dust > 0.05	1 hour
clean radiators panels	nuclear plant dust > 0.056	1 hour
fix structure segment 1	dome segment 1 damage > 0.05	1 hour
fix structure segment 2	dome segment 2 damage > 0.05	1 hour
fix structure segment 3	dome segment 3 damage > 0.05	1 hour
fix structure segment 4	dome segment 4 damage > 0.05	1 hour
fix structure segment 5	dome segment 5 damage > 0.05	1 hour

capacity.

Table 3 provides the cost associated with the relevant parameters describing the design space. Note that these values are provided in units of mass. It is common in space applications to consider equivalent system mass (ESM) [58], but ESM requires knowledge of mass, volume, crew time, power consumption, and cooling needs. Obtaining all of the values needed for those calculations is difficult as they are not publicly available. Thus, here we simply base our example costs on an estimate of the mass of each component. Commercially available hardware like solar panels is identified to serve as a basis for such calculations. Several different time periods are later used for the service life to consider how the service life affects design decisions.

For solar panels, we assume their mass follows a linear function based on energy generated. We assume a 0.093 m^2 panel weighs 1.22 kg [59] and has power output 12 W. Since the time unit is hours, we have: ($P_{\text{panel}} = \frac{12}{1.22}$ W/kg) plus the mass of the solar panel supports ($m_{\text{base}} = 10.76\ \text{kg}/\text{m}^2$). For estimating the mass of the nuclear reactor, we divide it into the nuclear plant, the nuclear material, and the fuel. We first subtract the mass of the nuclear plant from the nuclear reactor. As an estimate, the *Topaz-II* nuclear reactor [60] is used and its mass ($m_{\text{Topaz}} = 1061$ kg) is subtracted from the available cost and consider the energy of nuclear fuel as 24 GWhr/kg [61]. We also consider that 10^{-5} of the fuel is nuclear material, and the rest is not fuel or is not consumed completely. This calculation yields a very small number, but considering the dangers of transferring nuclear fuel and the special equipment required, it is a reasonable assumption. Finally, we assume the mass of the battery is represented by a linear function. The mass is determined based on existing Li-Ion batteries, with energy density of $E_{\text{bat.}} = 720000$ W/kg [62]. One complexity when dealing with solar batteries is their lifecycle. We assume that at the end of their life cycle ($t_{\text{Li-Ion}} = 1$year) the batteries may not be reliable enough to be used for the mission. Therefore, they require replacement every 5 years. Thus the total mission duration, t_{mission}, plays a role in determining the most appropriate design.

The other parameters for the sample habitat are chosen based on the assumption of having a dome with a scaled, 2.9 m radius, made of *concrete* [63] with 0.2 m thickness. The material used is based on assumptions about the

Table 3 Design variables and their costs

Parameter	Design Variable (kg)	Power/Energy	Unit
Power generation by solar cells during maximum solar irradiation	d_s	$P_{\text{panel}} \times (d_s + \frac{d_s}{m_{\text{base}}})$	W
Nominal production capacity of the nuclear plant	d_n	$P_{\text{nucl.}} \times \max(0\,\text{kg}, d_n - m_{\text{Topaz}})$	W
Power storage capacity	d_b	$E_{\text{bat.}} \times d_b \left\lceil \frac{t_{\text{mission}}}{t_{\text{Li-ion}}} \right\rceil$	J

properties of materials available on the Moon and the thickness value is chosen to prevent severe thermal fluctuations. The ECLSS temperature management module is modeled based on available design information [64] and its pressure management module similarly follows available design information [65].

C. Problem Formulation

The trade study considered herein is defined as choosing among multiple options for providing the energy for habitat's function and robotic agents' task. The design cost depends on the solar panel surface area d_s, the nuclear plant mass, d_n, and the battery capacity d_b – all expressed in terms of mass. If launch costs $r_{\text{launch}} = \$92,500$ /kg [66], we have:

$$c_0(d_s, d_n, d_b) = (d_s + d_n + d_b) r_{\text{launch}}.$$

When the interior conditions are acceptable and astronauts are available for conducting research, the habitat generates $r_{astronaut} = \$130,000\ /hour$ [67]. Let a_t be a variable taking the value one when the astronauts are available and zero otherwise. The interior environment is deemed acceptable when the temperature T_t is between $290°K$ and $300°K$ and the interior environment pressure P_t is between 0.7 atm and 1 atm. So, we define the value function by:

$$v(X_t) = 1_{[290°K, 300°K]}(T_t) 1_{[0.7\text{ atm}, 1\text{ atm}]}(P_t) a_t r_{\text{astronaut}}.$$

We set the discount factor to $\beta = 1$ simulate N_s

The next step in this process is setting the decision-making parameters. Since the performance of the system can improve, without adding any cost, by changing decisions regarding the repair tasks, we can add d_π to the list of variables.

Here d_π are the parameters that define the decision-making policy and π is the policy formed by them. Since these parameters are not referring to any physical parameters that are not bounded, they are not part of the constraint. The form of the policy model is arbitrary. It can use a rule-based expert system [68] (where the parameters of each rule are d_π) or it can be presented as an artificial neural network [69] (where the weights and biases form the d_π). In this example we consider a simpler approach using the priority of the actions.

We assume a static *time to failure* [70] as the parameters to model d_π. These parameters are defined for each task the agents need to do. The agents are assigned to the tasks with lower time to failure, since a lower time to failure

indicates less time to act before having catastrophic consequences. An equal time to failure value leads to a first in first out (FIFO) policy. The number of time to failure parameters is equal to the total number of possible tasks. This is the lowest number of decision-making related parameters for any decision-making model and helps us to solve for both hardware parameters (S, N, B) and time to failure simultaneously without getting skewed results due to the dominant nature of one of them.

V. Results and Discussion

Simulations are performed for a fifty-year habitat lifespan. We compared some samples based on a distribution based on fractional factorial sampling [71] for this study. The samples are mapped to a logarithmic space for the hardware-based parameters (S, N, B, d_π) to have a more diverse sampling focusing on points with extremely high and low samples. The maximum mass of design variables is $2,000$ kg for each design variable, which is able to provide required energy for ECLSS. The sampling procedure for the decision-making parameters are in linear scale and also follows fractional factorial method. These parameters indicate the priority of repairing tasks when the number of tasks exceeds number of available agents. Table 4 lists all possible values for each sample. Since we want the range of the values to be close to each other, we remove the samples with very different mass ratios between the components. For instance, cases with 2000 kg solar panel and 20 kg battery are removed to decrease the design size while keeping a consistent design approach in all variables. The decision-making parameters are listed in table 4 were applied on all component combinations.

Figure 5a shows the distribution of ENVP vs RNVP over these samples for a 50-year lifespan. The net value is calculated base on USD as explained in subsection IV.C. In this plot and all other results, we grouped the designs with similar total mass ranges. The designs with $c_0 < 200$ kg are grouped as blue, $c_0 \in [200, 1000]$ kg as green, $c_0 \in [1000, 3000]$ kg as orange, and $c_0 > 3000$ kg as red. The result shows that the mean and standard deviation of the net value are highly correlated and increase with increasing costs. We also report the distribution of mean and standard deviation of value in Figure 5b. Since the cost is negligible in this example compared to value, the plot of value and net value look quite similar. Thus, while the value (time spent doing science) is higher for the higher cost designs, and the

Table 4 Values used in habitat trade study for different design variables

Battery mass (kg)	Solar Panel mass (kg)	Nuclear mass (kg)	Repair dome	Clean Panel	Clean plant
20	20	0	2	1	1
100	100	-	1	2	1
300	300	-	1	1	2
1000	1000	-	1	1	1
2000	2000	2000	-		

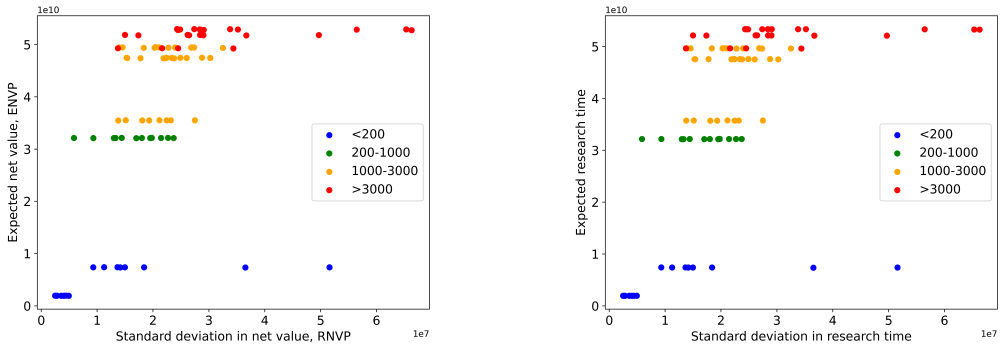

(a) Expected net value vs. Standard deviation in net value habitat design

(b) Expected Research time vs. standard deviation of research time for habitat design

Fig. 5 ENVP **vs.** RNVP **for habitat design**

effect of the cost seems to be overshadowed by the value term in this plot.

One important question to consider for design is which component has the most influence on the results. To investigate this question, we grouped the same designs based on the mass contributed by each component of the power subsystem rather than the total mass. These plots are shown in Figure 6. This figure demonstrates that the high value designs have a larger battery mass, but battery mass also has a more obvious correlation with higher ENVP. In other words, while all components may contribute to a suitable design, investing more toward battery mass is more important. Note that since we are not solving a constrained optimization, the best design uses the highest mass for each component. However, here we demonstrate how to also identify which particular component plays a more significant role.

The findings suggest that adding more battery mass is essential for improving performance, with a minimum of 1000 kg of battery mass being especially critical. This amount of battery mass may be sufficient for maintaining temperature and pressure while solar panels and nuclear plants are being repaired. In addition, the nuclear plant mass also appears to have a relatively clear effect on the results, although with only two possible weights for nuclear (0 kg and 2000 kg), the effect is less apparent than that of the batteries. While we did not quantify resilience in this study, the higher resilience of battery energy appears to be important due to the susceptibility of both nuclear plant radiators and solar panels to dust and the loss of functionality in solar panels during long Moon nights. Therefore, having a battery when these energy sources are not functioning is critical. However, relying solely on battery energy would be insufficient. An optimal energy component design for the habitat requires defining a total mass constraint and solving the optimization, which not specifically within the scope of this paper.

The choice of a decision policy may also be investigated with the CDCM as we next demonstrate. The impact of the choice of policy on distribution, as depicted in Figure 6d, is somewhat ambiguous, yet it provides some insight even in this simple example. Notably, allocating greater priority to dome repair is associated with higher uncertainty and larger RNVP values. This suggests that placing a high priority on the repair of the power subsystem components, which have a

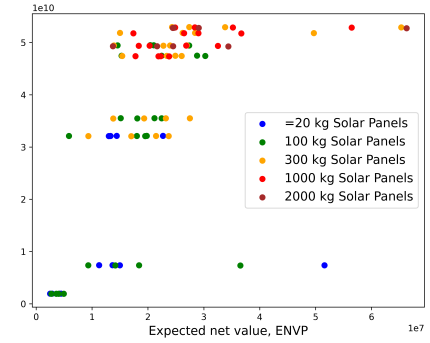

(a) Expected net value vs. Standard deviation in net value habitat design based on solar panel mass

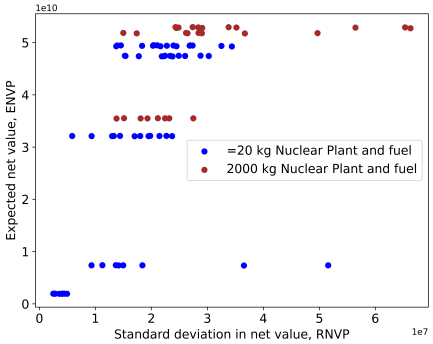

(b) Expected net value vs. Standard deviation in net value habitat design based on nuclear mass

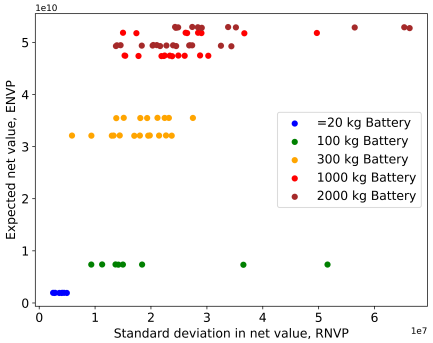

(c) Expected net value vs. Standard deviation in net value habitat design based on battery mass

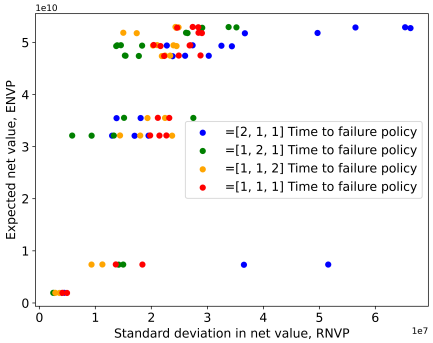

(d) Expected net value vs. Standard deviation in net value habitat design based on the policy

Fig. 6 Effect of different components on the total performance of the system

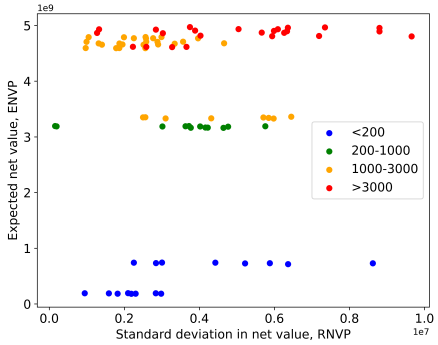

(a) Expected net value vs. Standard deviation in net value habitat design for a 5-year mission

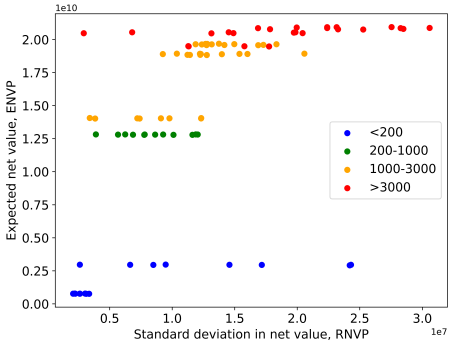

(b) Expected net value vs. Standard deviation in net value habitat design for a 20-year mission

Fig. 7 ENVP **vs.** RNVP **for habitat design for shorter missions**

more explicit connection to performance, leads to greater improvements in habitat temperature control. Conversely, prioritizing the cleaning of the nuclear plant has the lowest RNVP value, which is consistent with the anticipated effect based on Figure 6b.

Our study can also consider a variety of mission durations. Figures, 7a and 7b show the mean and standard deviations for missions with a 5-year and 20-year duration.

It is clear that the variation in the value of the designs, especially for the 5-year mission distribution, increases for shorter missions. Otherwise, the distribution looks quite similar to that of the previous figures that consider a 50-year mission. This result suggests that using the 50-year lifespan may be successfully extrapolated for longer missions.

Here we aim to present and illustrate the use of an easy-to-use framework for conducting trade studies that can provide early-stage evidence. While demonstration of the frame is the goal, the model is rather simple and thus limited, but can be augmented in the future for specific purposes, or trade studies where the goal is to understand the trends that influence the design choices. Modeling fidelity needs to be reduced to enable rapid simulations. To obtain this, the model requires striking a balance between the level of fidelity with the simulation speed.

VI. Conclusions

A new computational framework is developed for modeling and simulation the complex dynamics of interconnected systems of systems. Here we describe the architecture of the CDCM and demonstrate how to use it for different applications including making early design decisions. The CDCM is meant to provide the ability to run simulations that include complex scenarios involving several types of disruptions and disturbances, experience damage and degradation, capture consequences, and implement actions that support repair and recovery. Thus, in the architecture of the CDCM the execution code is separated from the system model to enable system models to be readily modified to represent different dynamical models and design configurations. The modular framework is thus convenient for evaluating the

performance of systems and for comparing design choices through performance metrics.

We apply the framework to two illustrative examples. The first example is meant to be relatively simple, and includes one building system experiencing both degradation and random earthquake events over its lifetime. The example illustrates the use of the CDCM for making a decision regarding the most appropriate maintenance period. The second example considers a lunar space habitat, including the power generation and storage subsystem, the structural subsystem, and a thermal control. The habitat is prone to four disturbances: solar radiation, dust that affects energy generation (solar and nuclear radiator panels), micrometeorite strikes, and exterior temperature fluctuations. The value of the habitat is represented by the time that is dedicated to performing science. The various disturbances and the repair actions therefore affect the performance of the habitat both directly and indirectly. The objective of this study is to select the most appropriate power generation and storage configuration. Different mission durations and decision policies are also investigated.

We are using the CDCM to perform specific trade studies, building on the explanations of the code provided herein. Throughout the development and initial use of this tool we learned several lessons. First, the models to be used to capture interconnected systems of systems such as space habitats must be selected deliberately to ensure that the relevant dynamics are included in the simulations, and yet the computation is not too demanding. This observation may mean that data-driven or other types of surrogate models are appropriate choices in many cases. Second, it will be beneficial to establish a model library with both the form of various models and the parameters applicable to specific hardware, enabling their reuse and exchange for trade studies. Third, measuring the performance in terms of the net value requires that one use common units for the value and cost terms, which is application-specific and requires careful consideration. Finally, users will find the code more attractive if more of the details of the execution are moved to the back end of the code. Thus, separating the system models from the execution is important.

Future versions of CDCM will enable rapid prototyping of systems-of-systems, and most importantly, abstractions upon which we can build individual components and systems are being developed to rapidly configure the reuse of those models. We are also building more capabilities on top of this, such as machine-readable casual models that will support a broader range of uses of the CDCM code.

Acknowledgments

This work was supported by a Space Technology Research Institutes Grant (number 80NSSC19K1076) from NASA's Space Technology Research Grants Program.

References

[1] Spagnulo, M., "Space Economy: A Business On the Launch Pad," *The Geopolitics of Space Exploration*, Springer, 2021, pp. 83–100.

[2] Schwartz, J. S., *The value of science in space exploration*, Oxford University Press, 2020.

[3] White, F., *The overview effect: Space exploration and human evolution*, AIAA, 1998.

[4] Clément, G., and Bukley, A. P., "Human space exploration–From surviving to performing," *Acta Astronautica*, Vol. 100, 2014, pp. 101–106.

[5] Chen, M., Goyal, R., Majji, M., and Skelton, R. E., "Review of space habitat designs for long term space explorations," *Progress in Aerospace Sciences*, Vol. 122, 2021, p. 100692.

[6] Bainbridge, W. S., "Motivations for space exploration," *Futures*, Vol. 41, No. 8, 2009, pp. 514–522.

[7] Smitherman, D. V., and Griffin, B. N., "Habitat concepts for deep space exploration," *AIAA Space 2014 Conference and Exposition*, 2014, p. 4477.

[8] Dyke, S. J., Marais, K., Bilionis, I., Werfel, J., and Malla, R., "Strategies for the design and operation of resilient extraterrestrial habitats," *Sensors and Smart Structures Technologies for Civil, Mechanical, and Aerospace Systems 2021*, Vol. 11591, International Society for Optics and Photonics, 2021, p. 1159105.

[9] Price, H., Baker, J., and Naderi, F., "A minimal architecture for human journeys to Mars," *New Space*, Vol. 3, No. 2, 2015, pp. 73–81.

[10] Cohen, M., "Mockups 101: Code and standard research for space habitat analogues," *AIAA SPACE 2012 Conference & Exposition*, 2012, p. 5153.

[11] Kennedy, K., "NASA Habitat Demonstration Unit Project-deep space habitat overview," *41st International Conference on Environmental Systems*, 2011, p. 5020.

[12] Howe, S. A., Kennedy, K. J., Gill, T. R., Smith, R. W., and George, P., "NASA habitat demonstration unit (HDU) deep space habitat analog," *AIAA Space 2013 conference and Exposition*, 2013, p. 5436.

[13] Ören, T., Zeigler, B. P., and Tolk, A., *Body of Knowledge for Modeling and Simulation: A Handbook by the Society for Modeling and Simulation International*, Springer Nature, 2023.

[14] Zeigler, B. P., Sarjoughian, H. S., Duboz, R., and Soulie, J.-C., *Guide to modeling and simulation of systems of systems*, Springer, 2013.

[15] Maria, A., "Introduction to modeling and simulation," *Proceedings of the 29th conference on Winter simulation*, 1997, pp. 7–13.

[16] Zeigler, B. P., Praehofer, H., and Kim, T. G., *Theory of modeling and simulation*, Academic press, 2000.

[17] Neto, V. V. G., Manzano, W., Rohling, A. J., Ferreira, M. G. V., Volpato, T., and Nakagawa, E. Y., "Externalizing patterns for simulations in software engineering of systems-of-systems," *Proceedings of the 33rd Annual ACM Symposium on Applied Computing*, 2018, pp. 1687–1694.

[18] Rohling, A. J., Neto, V. V. G., Ferreira, M. G. V., Dos Santos, W. A., and Nakagawa, E. Y., "A reference architecture for satellite control systems," *Innovations in Systems and Software Engineering*, Vol. 15, 2019, pp. 139–153.

[19] Manzano, W., Graciano Neto, V. V., and Nakagawa, E. Y., "Dynamic-sos: An approach for the simulation of systems-of-systems dynamic architectures," *The Computer Journal*, Vol. 63, No. 5, 2020, pp. 709–731.

[20] de França, B. B. N., and Travassos, G. H., "Experimentation with dynamic simulation models in software engineering: planning and reporting guidelines," *Empirical Software Engineering*, Vol. 21, No. 3, 2016, pp. 1302–1345.

[21] Santos, D. S., Oliveira, B. R., Kazman, R., and Nakagawa, E. Y., "Evaluation of systems-of-systems software architectures: state of the art and future perspectives," *ACM Computing Surveys*, Vol. 55, No. 4, 2022, pp. 1–35.

[22] Ferreira, F. H. C., Nakagawa, E. Y., and dos Santos, R. P., "Towards an understanding of reliability of software-intensive systems-of-systems," *Information and Software Technology*, Vol. 158, 2023, p. 107186.

[23] Heinicke, C., and Arnhof, M., "A review of existing analog habitats and lessons for future lunar and Martian habitats," *REACH*, Vol. 21, 2021, p. 100038.

[24] Vessey, W. B., Cromwell, R. L., and Platts, S., "NASA's Human Exploration Research Analog (HERA) for Studying Behavioral Effects of Exploration Missions," *Aerospace Medical Association (AsMA) Annual Scientific Meeting*, 2017.

[25] Penn, J., and Lin, A., "The Trick Simulation Toolkit: A NASA/Opensource Framework for Running Time Based Physics Models," *AIAA Modeling and Simulation Technologies Conference*, 2016, p. 1187.

[26] Detrell, G., Belz, S., and Keppler, J., "ELISSA: A Life Support System (LSS) technology selection, modelling and simulation tool for human spaceflight missions," *42nd COSPAR Scientific Assembly*, Vol. 42, 2018, pp. F4.3–5–18.

[27] Hendrickx, L., De Wever, H., Hermans, V., Mastroleo, F., Morin, N., Wilmotte, A., Janssen, P., and Mergeay, M., "Microbial ecology of the closed artificial ecosystem MELiSSA (Micro-Ecological Life Support System Alternative): reinventing and compartmentalizing the Earth's food and oxygen regeneration system for long-haul space exploration missions," *Research in microbiology*, Vol. 157, No. 1, 2006, pp. 77–86.

[28] Storek, T., Lohmöller, J., Kümpel, A., Baranski, M., and Müller, D., "Application of the open-source cloud platform FIWARE for future building energy management systems," *Journal of Physics: Conference Series*, Vol. 1343, IOP Publishing, 2019, p. 012063.

[29] Morstyn, T., Collett, K. A., Vijay, A., Deakin, M., Wheeler, S., Bhagavathy, S. M., Fele, F., and McCulloch, M. D., "OPEN: An open-source platform for developing smart local energy system applications," *Applied Energy*, Vol. 275, 2020, p. 115397.

[30] Documentation, S., "Simulation and Model-Based Design," , 2020. URL `https://www.mathworks.com/products/simulink.html`.

[31] Fritzson, P., *Principles of object-oriented modeling and simulation with Modelica 3.3: a cyber-physical approach*, John Wiley & Sons, 2014.

[32] "MS4 Modeling Environment," , 2024. URL https://www.ms4systems.com/pages/main.php.

[33] Cilli, M. V., and Parnell, G. S., "4.3. 1 Systems Engineering Tradeoff Study Process Framework," *INCOSE International Symposium*, Vol. 24, Wiley Online Library, 2014, pp. 313–331.

[34] Ackoff, R. L., "Towards a system of systems concepts," *Management science*, Vol. 17, No. 11, 1971, pp. 661–671.

[35] Groen, E. A., Heijungs, R., Bokkers, E. A., and De Boer, I. J., "Methods for uncertainty propagation in life cycle assessment," *Environmental Modelling & Software*, Vol. 62, 2014, pp. 316–325.

[36] Liu, X., Behjat, A., Dyke, S., Whitaker, D., Ramirez, J., and Bilionis, I., "Roles of Human and Robotic Agents Toward Operating a Smart Space Habitat," 2023 International Conference on Environmental Systems, 2023.

[37] Liu, X., Behjat, A., Dyke, S. J., Whitaker, D., Ramirez, J., and Bilionis, I., "The Future of Smart Space Habitats: Comparing Humans with Robots," *AIAA Journal*, in review.

[38] Cilento, M. V., "Resilient Extra-Terrestrial Habitat Design Using a Control Effectiveness Metric," Ph.D. thesis, Purdue University Graduate School, 2022.

[39] De Oliveira, M., Lima, V. M., Yamashita, S. M. A., Alves, P. S., and Portella, A. C., "Experimental planning factorial: a brief review," *International Journal of Advanced Engineering Research and Science*, Vol. 5, No. 6, 2018, p. 264164.

[40] Mockus, J., *Bayesian approach to global optimization: theory and applications*, Vol. 37, Springer Science & Business Media, 2012.

[41] Solomatine, D. P., and Ostfeld, A., "Data-driven modelling: some past experiences and new approaches," *Journal of hydroinformatics*, Vol. 10, No. 1, 2008, pp. 3–22.

[42] Sanner, M. F., et al., "Python: a programming language for software integration and development," *J Mol Graph Model*, Vol. 17, No. 1, 1999, pp. 57–61.

[43] Neely, A., Gregory, M., and Platts, K., "Performance measurement system design: a literature review and research agenda," *International journal of operations & production management*, Vol. 15, No. 4, 1995, pp. 80–116.

[44] Yodo, N., and Wang, P., "Engineering resilience quantification and system design implications: A literature survey," *Journal of Mechanical Design*, Vol. 138, No. 11, 2016, p. 111408.

[45] Uday, P., and Marais, K., "Designing resilient systems-of-systems: A survey of metrics, methods, and challenges," *Systems Engineering*, Vol. 18, No. 5, 2015, pp. 491–510.

[46] Alonso-Rasgado, T., Thompson, G., and Elfström, B.-O., "The design of functional (total care) products," *Journal of engineering design*, Vol. 15, No. 6, 2004, pp. 515–540.

[47] (ICC), I. C. C., 2021. URL https://codes.iccsafe.org/content/IBC2021P1.

[48] of Civil Engineers, A. S., "Minimum design loads and associated criteria for buildings and other structures," American Society of Civil Engineers, 2017.

[49] "CESMD," , 2023. URL https://www.strongmotioncenter.org/cgi-bin/CESMD/iqr_dist_DM2.pl?iqrid=losangelesairport_25jul2012_15182841&SFlag=0&Flag=2.

[50] "Structural Engineering Software," , 2022. URL https://www.csiamerica.com/products/sap2000/enhancements/17.

[51] Committee, A., "Building code requirements for structural concrete (ACI 318-08) and commentary," American Concrete Institute, 2008.

[52] Kaczmarzyk, M., Gawronski, M., and Piatkowski, G., "Global database of direct solar radiation at the Moon's surface for lunar engineering purposes," *E3S Web of Conferences*, Vol. 49, EDP Sciences, 2018, p. 00053.

[53] Chin, G., Brylow, S., Foote, M., Garvin, J., Kasper, J., Keller, J., Litvak, M., Mitrofanov, I., Paige, D., Raney, K., et al., "Lunar reconnaissance orbiter overview: Theáinstrument suite and mission," *Space Science Reviews*, Vol. 129, No. 4, 2007, pp. 391–419.

[54] Laloui, L., and Rotta Loria, A. F., "Chapter 3 - Heat and mass transfers in the context of energy geostructures," *Analysis and Design of Energy Geostructures*, edited by L. Laloui and A. F. Rotta Loria, Academic Press, 2020, pp. 69–135. https://doi.org/https://doi.org/10.1016/B978-0-12-816223-1.00003-5, URL https://www.sciencedirect.com/science/article/pii/B9780128162231000035.

[55] Jiang, J., Main, J. A., Weigand, J. M., and Sadek, F. H., "Thermal performance of composite slabs with profiled steel decking exposed to fire effects," *Fire safety journal*, Vol. 95, 2018, pp. 25–41.

[56] Keste, A., and Patil, S., "Investigation of concrete solar collector: a review," *IOSR J. Mech. Civ. Eng*, Vol. 6, 2012, pp. 26–29.

[57] Yun, T. S., Jeong, Y. J., and Youm, K.-S., "Effect of surrogate aggregates on the thermal conductivity of concrete at ambient and elevated temperatures," *The Scientific World Journal*, Vol. 2014, 2014.

[58] Levri, J., Fisher, J. W., Jones, H. W., Drysdale, A. E., Ewert, M. K., Hanford, A. J., Hogan, J. A., Joshi, J., Vaccari, D. A., et al., "Advanced life support equivalent system mass guidelines document," Tech. rep., NASA, 2003.

[59] Brandhorst Jr, H. W., and Spakowski, A. E., "A 23.4 square-foot/2.17-SQ-M/cadmium sulfide thin-film solar cell array," Tech. rep., 1968.

[60] Voss, S. S., "Topaz II System Description," Tech. rep., Los Alamos National Lab., 1994.

[61] "Euronuclear Fuel-Comparison," https://www.euronuclear.org/glossary/fuel-comparison/, 2022. Accessed: 2022-02-01.

[62] Zhang, C., Yang, X., Ren, W., Wang, Y., Su, F., and Jiang, J.-X., "Microporous organic polymer-based lithium ion batteries with improved rate performance and energy density," *Journal of Power Sources*, Vol. 317, 2016, pp. 49–56.

[63] McKay, D. S., Heiken, G., Basu, A., Blanford, G., Simon, S., Reedy, R., French, B. M., and Papike, J., "The lunar regolith," *Lunar sourcebook*, Vol. 567, 1991, pp. 285–356.

[64] "1.5 ton AC, 45,000 BTU 96% Afue Gas Furnace, 15.5 Seer Horizontal split system kit," , 2022. URL https://www.alpinehomeair.com/product/air-conditioning-cooling/central-heating-cooling-complete-systems/blueridge/ba16l18p-bg961uh045be12-bh1p30b.

[65] "Quick links," , 2022. URL https://www.dewalt.ca/product/d55154/11-hp-continuous-4-gallon-electric-wheeled-dolly-style-air-compressor-panel.

[66] Jones, H., "Equivalent mass versus life cycle cost for life support technology selection," *33nd International Conference on Environmental Systems*, 2003.

[67] Foust, J., "NASA hikes prices for commercial ISS users," , Jan 2023. URL https://spacenews.com/nasa-hikes-prices-for-commercial-iss-users/.

[68] Abraham, A., "Rule-Based expert systems," *Handbook of measuring system design*, 2005.

[69] Wang, S.-C., "Artificial neural network," *Interdisciplinary computing in java programming*, Springer, 2003, pp. 81–100.

[70] McPherson, J. W., *Reliability physics and engineering: time-to-failure modeling*, Springer, 2018.

[71] Oles, P. J., "Fractional factorial design approach for optimizing analytical methods," *Journal of AOAC International*, Vol. 76, No. 3, 1993, pp. 615–620.

Appendix: Models implemented in the Illustrative example

Table 5 Structural subsystem parameters.

Attributes	Notation	Description
name	ST	
id	2	
coupling inputs	$X^0_{5,t}$	interior environment temperature
control inputs	$A^0_{2,t}$	repair damage in section 1
	$A^1_{2,t}$	repair damage in section 2
	$A^2_{2,t}$	repair damage in section 3
	$A^3_{2,t}$	repair damage in section 4
	$A^4_{2,t}$	repair damage in section 5
external disturbances	Ω^1_t	solar irradiation
	Ω^2_t	external environment temperature
	Ω^3_t	micrometeorite impact in section 1
	Ω^4_t	micrometeorite impact in section 2
	Ω^5_t	micrometeorite impact in section 3
	Ω^6_t	micrometeorite impact in section 4
	Ω^7_t	micrometeorite impact in section 5
states	$X^0_{2,t}$	structure external side temperature
	$X^1_{2,t}$	structure internal side temperature
	$X^2_{2,t}$	damage in section 1
	$X^3_{2,t}$	damage in section 2
	$X^4_{2,t}$	damage in section 3
	$X^5_{2,t}$	damage in section 4
	$X^6_{2,t}$	damage in section 5
parameters	θ^0_2	nominal thermal conductivity (k/d)
	θ^1_2	severely damaged thermal conductivity(k/d)
	θ^2_2	external environment pressure
	θ^3_2	convection heat transfer coefficient inside
	θ^4_2	surface absorptivity coefficient
	θ^5_2	Stefan-Boltzmann coefficient surface emissivity
	θ^6_2	ground isolation emissivity
	θ^7_2	dome external surface area
	θ^8_2	dome ground surface area
coupled parameters	-	-

Table 6 [continuation] Structural subsystem parameters.

Functions	Notation
state transition functions	$X^0_{2,t+1} = X^0_{2,t} +$
	$\left(\left(X^1_{2,t} - X^0_{2,t}\right\} \times \left((1 - \bar{X}^{2,\cdots,6}_{2,t})\theta^1_2 + \bar{X}^{2,\cdots,6}_{2,t}\theta^0_2\right\} +$
	$\left(\theta^4_2(\Omega^2_t)^4 - \theta^6_2(X^0_{2,t})^4\right\} \times \theta^5_2 +$
	$\Omega^1_t \Big/ \theta^2_2$
	$X^1_{2,t+1} = X^1_{2,t} +$
	$\left(\left(X^0_{2,t} - X^1_{2,t}\right\}\left((1 - \bar{X}^{2,\cdots,6}_{2,t})\theta^1_2 + \bar{X}^{2,\cdots,6}_{2,t}\theta^0_2\right\} +$
	$\left(X^0_{5,t} - X^1_{2,t}\right\} \times \theta^3_2\right\}\Big)/\theta^2_2$
	$X^2_{2,t+1} = \min\left\{\max\left\{(X^2_{2,t} - f(\Omega^3_t) + A^0_{2,t}, 0\right\}, 1\right\}$
	$X^3_{2,t+1} = \min\left\{\max\left\{(X^3_{2,t} - f(\Omega^4_t) + A^1_{2,t}, 0\right\}, 1\right\}$
	$X^4_{2,t+1} = \min\left\{\max\left\{(X^4_{2,t} - f(\Omega^5_t) + A^2_{2,t}, 0\right\}, 1\right\}$
	$X^5_{2,t+1} = \min\left\{\max\left\{(X^5_{2,t} - f(\Omega^6_t) + A^3_{2,t}, 0\right\}, 1\right\}$
	$X^6_{2,t+1} = \min\left\{\max\left\{(X^6_{2,t} - f(\Omega^7_t) + A^4_{2,t}, 0\right\}, 1\right\}$

Table 7 Power subsystem parameters.

Attribute	Notation	Description	Value	Unit
name	PG			
id	3			
coupling inputs	$X^0_{4,t}$	power consumption for temperature control	-	J
	$X^1_{4,t}$	power consumption for pressure control	-	J
control inputs	$A^0_{3,t}$	cover solar panel	-	-
	$A^1_{3,t}$	clean solar panel dust	-	-
	$A^2_{3,t}$	clean nuclear dust	-	-
external disturbances	Ω^0_t	dust deposition rate	$\in [0,\ 1]$	-
	Ω^1_t	solar irradiation	-	$\frac{\mathrm{W}}{\mathrm{m}^2}$
states	$X^0_{3,t}$	covered/uncovered	$\in \{0,\ 1\}$	-
	$X^1_{3,t}$	generated solar energy	-	J
	$X^2_{3,t}$	generated nuclear energy	-	J
	$X^3_{3,t}$	generated power total	-	J
	$X^4_{3,t}$	energy storage level	-	J
	$X^5_{3,t}$	cleanness from dust of solar	$\in [0,\ 1]$	-
	$X^6_{3,t}$	cleanness from dust of nuclear	$\in [0,\ 1]$	-
parameters	θ^0_3	solar cells efficiency	30%	-
	θ^1_3	solar cells capacity	-	$\frac{\mathrm{W}}{\mathrm{m}^2}$
	θ^2_3	nominal production capacity of the nuclear fuel	$864E9$	$\frac{\mathrm{J}}{\mathrm{kg}}$
	θ^3_3	power storage capacity	720000	$\frac{\mathrm{J}}{\mathrm{kg}}$
coupled parameters	-	-		
Functions		Notation		
state transition functions		$X^0_{3,t+1} = A^0_{3,t}$	$\in \{0,\ 1\}$	-
		$X^1_{3,t+1} = \max((X^0_{3,t} \times X^5_{3,t} \times \Omega^1_t \times \theta^0_3 \times \theta^1_3), 0)$	-	J
		$X^2_{3,t+1} = \max((X^6_{3,t} \times \theta^2_3), 0)$	-	J
		$X^3_{3,t+1} = X^1_{3,t} + X^2_{3,t}$	-	J
		$X^4_{3,t+1} = \min(\max(X^4_{3,t} + X^3_{3,t} - X^0_{4,t} - X^1_{4,t}), 0), \theta^3_3)$	-	J
		$X^5_{3,t+1} = \min(\max(X^5_{3,t} - X^5_{3,t}\Omega^0_t + A^2_{3,t}, 0), 1)$	$\in [0,\ 1]$	-
		$X^6_{3,t+1} = \min(\max(X^6_{3,t} - \Omega^0_t + A^1_{3,t}, 0), 1)$	$\in [0,\ 1]$	-

Table 8 Environmental control and life support subsystem parameters.

Attribute	Notation	Description	Value	Unit
name	ES			
id	4			
coupling inputs	$X^0_{5,t}$	interior environment temperature	-	K
	$X^1_{2,t}$	structure internal side temperature	-	K
	$X^3_{3,t}$	power storage level	-	J
	$X^{2,\cdots,6}_{2,t}$	structure damage	$\in [0,\ 1]$	-
control inputs	-	-		
external disturbances	-	-		
states	$X^0_{4,t}$	power needed for temperature control	-	J
	$X^1_{4,t}$	power needed for pressure control	-	J
	$X^2_{4,t}$	power consumption for temperature control	-	J
	$X^3_{4,t}$	power consumption for pressure control	-	J
parameters	θ^0_4	nominal efficiency of the TM	12.5	-
	θ^1_4	nominal efficiency of the PM	31.25	$\frac{\text{J}}{\text{atm}}$
	θ^2_4	specific heat capacity air	1003.5	$\frac{\text{J}}{\text{kgK}}$
	θ^3_4	air leakage coefficient	0.01	$\frac{\text{atm}}{\text{s}}$
	θ^4_4	pressure control energy	1000	J
coupled parameters	θ^2_2	external environment pressure	0	atm
	θ^0_5	set point temperature for interior environment	300	K
	θ^1_5	set point pressure for interior environment	1.0	atm
Functions		Notation		
physical state transition functions		$X^0_{4,t+1} = \left\lvert \left(\theta^0_5 - X^0_{5,t} \right) \theta^2_{4,t} - \left(X^1_{2,t} - X^0_{5,t} \right) \theta^3_2 \right) \Big/ \theta^0_{4,t} \right\rvert$	-	J
		$X^1_{4,t+1} = \left\lvert \left((\theta^1_5 - X^1_{5,t}) \times \theta^4_4 - (\theta^9_2 - X^1_{5,t})(1 - \bar{X}^{2,\cdots,6}_{2,t}) \theta^3_4 \right) \right) \Big/ \theta^1_4 \right\rvert$	-	J
		$X^2_{4,t+1} = \max \left(0, \min \left\{ X^3_{3,t} - X^1_{4,t}, X^0_{4,t} \right\} \right)$	-	J
		$X^3_{4,t+1} = \max \left(0, \min \left\{ X^3_{3,t}, X^1_{4,t} \right\} \right)$	-	J

Table 9 Interior environment model parameters.

Attribute	Notation	Description	Value	Unit
name	IE			
id	5			
coupling inputs	$X^0_{4,t}$	power consumption for temperature control		
	$X^1_{4,t}$	power consumption for pressure control	-	J
	$X^2_{4,t}$	power needed for temperature control	-	J
	$X^3_{4,t}$	power needed for pressure control	-	J
	$X^1_{2,t}$	internal structural temperature	-	J
	$\bar{X}^{2,\cdots,6}_{2,t}$	structure latent health	$\in [0,\ 1]$	-
control input	-	-		
external disturbances	-	-		
states	$X^0_{5,t}$	interior environment temperature	-	K
	$X^1_{5,t}$	interior environment pressure	-	atm
parameters	θ^0_5	set point temperature for interior environment	-	K
	θ^1_5	set point pressure for interior environment	-	atm
	θ^2_5	air leakage coefficient	-	-
coupled parameters	θ^3_2	convection heat transfer coefficient	-	$\frac{\mathrm{W}}{\mathrm{m^2K}}$
	θ^2_2	external environment pressure	-	atm
Functions		Notation		
physical state transition functions		$X^0_{5,t+1} = \frac{X^0_{4,t}}{X^2_{4,t}}\theta^0_5 + (1 - \frac{X^0_{4,t}}{X^2_{4,t}})X^1_{2,t}$	-	K
		$X^1_{5,t+1} = \frac{X^1_{4,t}}{X^3_{4,t}}\theta^1_5 + (1 - \frac{X^1_{4,t}}{X^3_{4,t}})\theta^9_2\theta^2_5(1 - \bar{X}^{2,\cdots,6}_{2,t})$	-	atm